THESIS

EXPLORING THE ROLES OF BZZ1 IN CLATHRIN-MEDIATED ENDOCYTOSIS

Submitted by

Lauren Marie Barry

Department of Biochemistry and Molecular Biology

In partial fulfillment of the requirements

For the Degree of Master of Science

Colorado State University

Fort Collins, Colorado

Spring 2015

Master's Committee:

Advisor: Santiago Di Pietro

Norm Curthoys
Frances Glycenfer

ABSTRACT

EXPLORING THE ROLES OF BZZ1 IN CLATHRIN-MEDIATED ENDOCYTOSIS

Clathrin-mediated endocytosis (CME) is a highly conserved process in eukaryotes. This particular route of endocytosis plays an integral role in virus internalization, nutrient uptake, regulation of signal transduction, and overall cell health. CME can be characterized by three distinct stages: coat formation, cargo binds a receptor on the plasma membrane which leads to the recruitment of coat proteins and the formation of a clathrin coated pit; actin polymerization, globular actin will polymerize in such a way that the vesicle can overcome the turgor pressure of the plasma membrane; and scission and coat disassembly, the vesicle is separated from the plasma membrane and the coat proteins are recycled for the next endocytic event. Initiation of actin polymerization is mediated by the activation of the Arp2/3 complex. Arp2/3 is activated by Las17, the yeast homolog of human WASp (Wiskott-Aldrich Syndrome protein). Las17 interacts with multiple proteins, both activators and inhibitors. The activity of Las17 is inhibited by a protein called Sla1. Sla1 binds the P8-12 region of Las17 and blocks one of two globular actin binding sites. Sla1 and Las17 form a stable complex referred to as SLAC (Sla1, Las17, Actin, and Clathrin) and arrive at the plasma membrane together. This project deals specifically with the interaction between the SLAC complex and the putative activator Bzz1 and explores the possibility that Bzz1 both activates actin polymerization and tubulates the plasma membrane. Understanding the mechanisms that allow clathrin-mediated endocytosis to progress from start to finish is critical. Wiskott-Aldrich Syndrome, hypercholesterolemia, and neurodegenerative disorders can all be tied to defects in CME.

ACKNOWLEDGEMENTS

A special thanks to Dr. Santiago Di Pietro for recognizing my potential as an undergrad and providing me with every possible resource to succeed since then. You pushed me to a higher standard and I am so very grateful for that. I would also like to thank Dr. Daniel Feliciano who got me started on this project and taught me how to think critically and creatively. To Kristen Farrell, without whom I would not have survived in the lab after the departure of my original mentor. To Tommy Tolsma, for his keen attention to detail and insightful questions. To Dr. Andrea Ambrosio, for being an expert in all the things I find most confusing. To Al Aradi for surviving pyrene-actin polymerization assays with me.

I would also like to thank my committee members as well as staff members for taking the time to teach me and critique my work.

Finally, I would like to thank my family. Their unending support and encouragement has been invaluable to my journey as a scientist.

TABLE OF CONTENTS

LIST OF FIGURES

INTRODUCTION

Actin polymerization is a crucial step in clathrin-mediated endocytosis. It provides the force necessary for a clathrin coated vesicle to be internalized. A considerable amount of research has been done to illuminate how the actin polymerization step of CME is regulated; however, researchers have yet to explain how Las17 is activated at the start of actin polymerization.

Yeast as a Model System for Clathrin-mediated Endocytosis

The proteins described in this research are from *Saccharomyces cerevisiae*, or budding yeast. It is often difficult for the general population to appreciate research when it cannot be applied to humans and human diseases. However, CME is a conserved process from yeast to humans. Thus, discoveries made in yeast can be applied to humans and eventually have clinical applications as well. Using yeast for research has many obvious advantages (i.e. quick multiplying time, low cost, high resiliency, easy manipulation of genome, collections of knock out and GFP-tagged strains, etc.). A well-defined sequence of events has been established in yeast clathrin-mediated endocytosis using fluorescent microscopy which makes it easier for researchers in this field to understand exactly what is happening from a temporal perspective (3). Further, recent publications using genome-edited mammalian cells demonstrated the same sequence of events as first observed in yeast cells (4).

Clathrin-mediated Endocytosis

Clathrin-mediated endocytosis, also known as receptor-mediated endocytosis, can be characterized by the presence and function of over fifty proteins. In particular, clathrin is the coat protein that sets CME apart from other types of endocytosis and vesicle trafficking. The smallest subunit of clathrin is the triskelion which polymerizes to form a basket that facilitates

vesicle budding (Figure 1). Clathrin depends on adaptor proteins to link it to cargo-bound receptors. Clathrin-mediated endocytosis allows cells to take up nutrients, communicate, and respond to the environment. Defects in CME can severely affect the health of a cell and can lead to hypercholesterolemia, immune deficiencies, and neurodegenerative disorders in humans.

Actin

CME was linked to the actin cytoskeleton by an experiment that utilized Latrunculin-A, an actin depolymerizing drug, to show that without actin polymerization clathrin coated pits are virtually immobilized at the plasma membrane (5, 15). Actin is essential for many processes inside the cell. Intermediate filaments, microtubules, and microfilaments (made from actin), are all essential for a healthy cytoskeleton. In yeast, actin forms the actomyosin ring which is needed during cell division, actin cables which are used for cell motility and intracellular transport, and cortical actin patches which are created in the interest of clathrin-mediated endocytosis (12). Actin exists in a globular form (G-actin) and a filamentous form (F-actin). Although actin polymerization can be triggered *in vitro* using high salt concentrations, it requires the help of a variety of proteins to polymerize *in vivo.*

Arp2/3 Complex

The Arp2/3 complex stimulates the formation of a branched actin network. Subunit 2 and subunit 3 mimic monomeric actin; thus, providing a nucleation site for new actin filaments. However, Arp2/3 typically uses an existing filament to bind and polymerize actin at a 70 degree angle from that very filament (14). Arp2/3 is not active alone. It exists in an inactive conformation without the presence of nucleation promoting factors (NPFs).

Las17

Yeast have five different nucleation promoting factors: Las17, Myo3, Myo5, Pan1, and

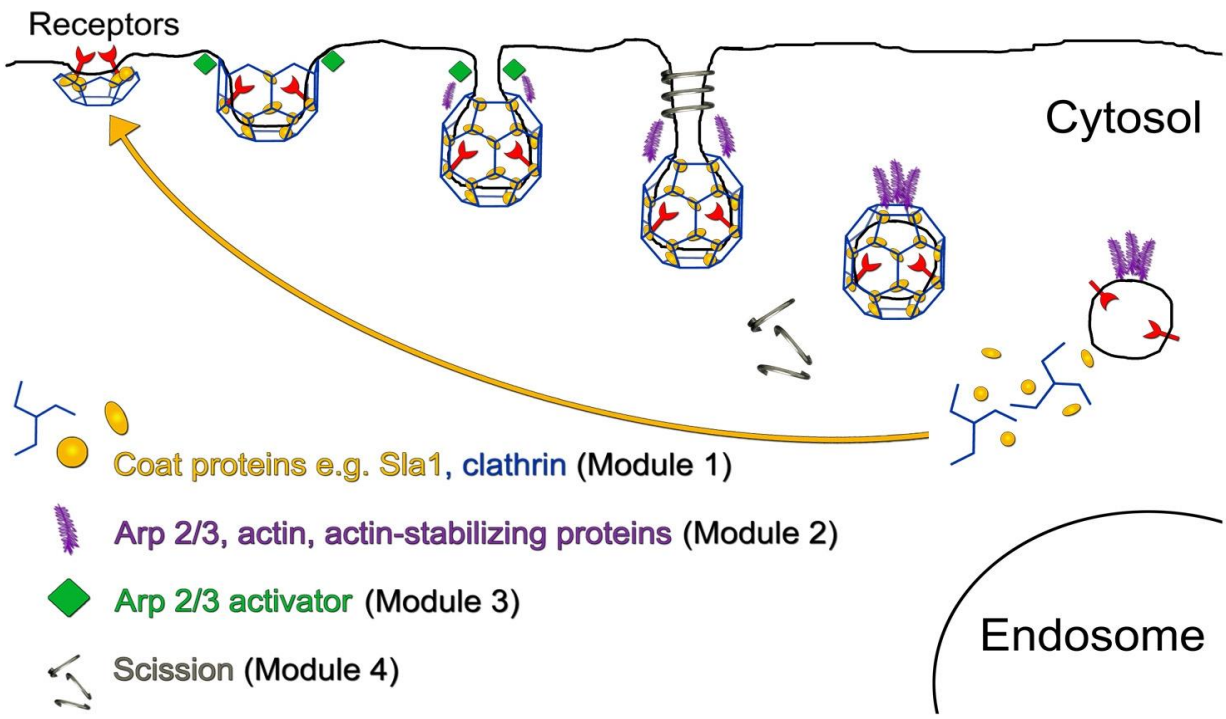

Figure 1. Model of clathrin-mediated endocytosis. Coat formation, actin polymerization, and scission and coat disassembly are pictured.

Abp1. Las17 has the strongest activity of all of these NPFs (9, 21, 22). Mutations in the mammalian homolog of Las17, WASp, are the cause of Wiskott-Aldrich Syndrome, a genetic disorder that leads to eczema, low platelet count, and immune deficiencies. From its N to C-terminus, Las17 contains a WASp Homology 1 (WH1) domain, a polyproline domain, a WASp Homology 2 (WH2) domain, and an acidic tail (Figure 2A). The ability Las17 has to bind G-actin categorizes it as a class 1 NPF. The WH2 domain and the acidic tail comprise what is known as the WCA domain (WH2/Central/Acidic) which binds both G-actin and the Arp2/3 complex (12, 13, 15, 17, 19). Recently, a select set of arginine residues in the P8-12 region of Las17 have also been shown to bind G-actin. This site has been termed the Las17 G-actin binding motif (LGM) (8). Therefore, the high nucleation function of Las17 can be attributed to its two G-actin binding sites. Las17 is heavily responsible for initiation of actin polymerization during CME; however, it arrives at the cortical actin patch about twenty seconds before actin filaments are detected. This activity is heavily regulated by number of other proteins.

Sla1

Sla1 is a coat protein that inhibits the NPF capacity of Las17. From its N to C terminus, Sla1 contains three SH3 domains which bind polyproline motifs (PxxPs), a Sla1 homology domain 1 (SHD1), a polyproline domain, a Sla1 homology domain 2 (SHD2), a clathrin binding motif (LLDLQ), and a sequence of TGGxxPQ repeats which are thought to play a role in organizing the actin network (2, 10) (Figure 2B). Sla1 can be considered an adaptor protein as its structure contains domains important for both cargo recruitment (SHD1) and clathrin binding (LLDLQ). Las17 and Sla1 form a stable complex referred to as the SLAC (Sla1, Las17, Actin, and Clathrin) complex. A group of polyproline motifs (P8-12) in Las17 form a strong, direct interaction with the first two SH3 domains of Sla1 (7). Although Sla1 does not act alone in its

inhibition of Las17, it effectively blocks G-actin binding at the LGM. In this way actin polymerization does not occur prematurely. What remains unclear is how this inhibition is relieved to allow actin polymerization. One possibility is that other proteins relieve this inhibition and allow CME to progress.

Bzz1

From its N to C terminus, Bzz1 contains an FCH-BAR (F-BAR) domain, a linker domain, and two SH3 domains with a short linker in between (Figure 2C). Published data suggests the idea that Bzz1 activates the SLAC complex. For instance, Bzz1 arrives after Las17 but only a short period before Abp1, a marker for the onset of actin polymerization. *In vitro*, pyrene-actin polymerization assays have also shown that the loss of polymerization accompanied by the addition of Sla1 to Las17, Arp2/3, and actin can be recovered by the addition of full length Bzz1 (22). The mechanism for this activation is unknown. It could be that Bzz1 SH3 domains bind to Las17 and disassemble or open up the SLAC complex. It is also not known whether Bzz1 activates Las17 *in vivo.* It is known that F-BAR domains can dimerize. This could either allow Bzz1 to gather two molecules of Las17 together, thereby multiplying the NPF effects of Las17, or it may enable another mechanism of activation that will be described in the results and discussion sections.

F-BAR domains can also bind and tubulate the plasma membrane. The slightly concave structure in addition to an enrichment of basic residues give F-BAR domains a unique affinity for negatively charged phospholipids in the inner leaflet of the lipid bilayer (13). Syndapin, the mammalian homolog of Bzz1, provides possible clues to the mechanism by which Bzz1 could link activation of actin polymerization to membrane binding and tubulation. The SH3 domain of

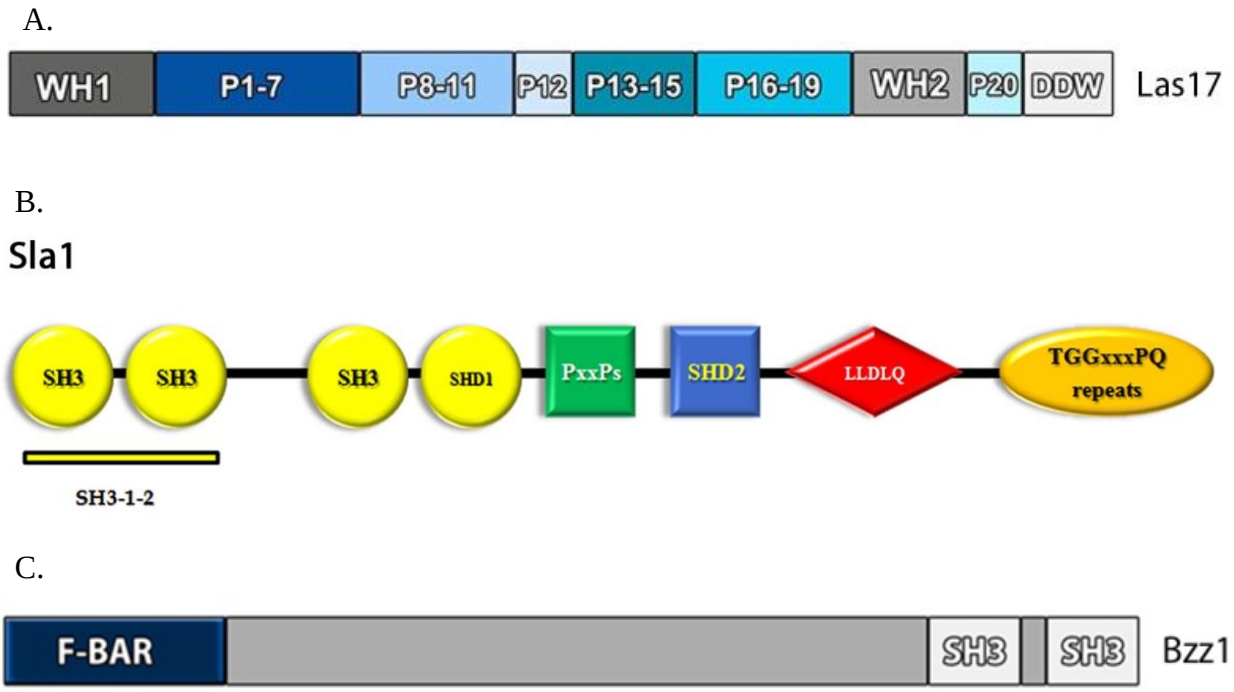

Figure 2. Illustrations of Las17, Sla1, and Bzz1. (A) The various domains of Las17 are shown. (B) The various domains of Sla1 are shown. (C) The various domains of Bzz1 are shown.

Syndapin auto inhibits the tubulation function of the F-BAR domain. Once the SH3 domain of Syndapin is bound and occupied by Dynamin, a mammalian GTPase that aides in vesicle scission, Syndapin adopts an open, active conformation that allows the F-BAR domains to assist in supporting the membrane curvature (18). If Bzz1 does indeed behave like Syndapin it is possible that it helps the progression of CME by coupling membrane tubulation with actin polymerization.

Few hypotheses have been made about how Bzz1 activates Las17 and by extension actin polymerization. The goal of the following research has been to illuminate a likely mechanism by which this occurs and provide original data that supports that mechanism.

RESULTS

Characterizing the Interaction between Las17 and Bzz1

Other labs have shown that the SH3 domains of Bzz1 bind Las17; however, none have shown the specific residues of Las17 that participate in this interaction and how strong the interaction is. Yeast two-hybrid assays were carried out with the SH3 domains of Bzz1 and different segments of the polyproline domain of Las17 which can be separated into twenty discrete PxxP motifs (7) (Figure 2A). Each polyproline motif consists of a proline, two variable amino acids, and another proline. Cell growth in media lacking Histidine (-His) indicates interaction between the two proteins. Two fragments of the polyproline domain (P1-7 and P8-11) exhibited growth in –His media (Figure 3A). The interaction between P1-7 and Bzz1 persists even in the presence of 5 mM 3-AT, indicating a strong interaction. The interaction between P8-11 and Bzz1 persists in the presence of 1 mM 3-AT, indicating a moderate strength interaction. To confirm this result and show that the interaction between these two proteins is direct, a GST pulldown with purified proteins was performed. GST-P1-7 and GST-P8-11 were immobilized by binding to glutathione beads and incubated with equal amounts of poly-Histidine tagged Bzz1 SH3 domains 1 and 2 (Bzz1 SH3 1-2). Bound Bzz1 SH3 1-2 was detected by immunoblotting using anti-His antibodies. The P1-7 fragment binds Bzz1 SH3 domains with a higher affinity than the P8-11 fragment, yet both interactions are significant when compared to the GST negative control (Figure 3B). Strong binding to the P1-7 fragment can be attributed to P1. Another GST pulldown demonstrates that when P1 is mutated, the majority of the interaction between Las17 and Bzz1 is lost (Figure 3C).

The partial overlap in Las17 binding sites between Sla1 (P8-12) and Bzz1 (P8-11) led us to believe that Bzz1 and Sla1 may compete for binding to Las17. A ligand depletion assay was

used to determine the binding affinity between Las17 (P1-12) and Bzz1. 0, 0.1, 0.2, 0.5, 1.5, and 4 μM concentrations of a GST tagged P1-12 fragment of Las17 were bound to glutathione beads in a 500 μL reaction. After washing, a 1.5 μM concentration of poly-Histidine tagged Bzz1 full length was allowed to bind. Samples of the supernatant, representing the unbound fraction, were collected and analyzed by SDS-PAGE (Figure 3D). At a K_D of 0.2 ± 0.01 μM, the affinity of Bzz1 for Las17 was notable, but about four times less than that of Sla1 for Las17, K_D 56.0 ± 8.0 nM (7). This evidence discourages a model that involves competition, because Bzz1 would lose out against the strong interaction taking place in the SLAC complex, especially since the P8-12 region is not the main binding site for Bzz1. Moreover, if the primary mode of activation of actin polymerization by Bzz1 is competing with Sla1 for the G-actin binding site, then it is more probable that Bzz1 would further inhibit Las17, which we know is not the case.

Bzz1 Binds Las17 without Inducing SLAC Dissociation

To further test the idea that Bzz1 activates the SLAC complex by competitively binding to Las17 and displacing Sla1, another GST pulldown was used. 0.5 μM of GST-Las17 P1-12 was bound to glutathione beads in a 500 μL reaction. Las17 was saturated with 4 μM of poly-Histidine tagged Sla1 SH3 domains. The beads were washed and 0, 2, and 5 μM concentrations of poly-Histidine tagged Bzz1 full length were added and allowed to bind. Interestingly, while increasing the concentration of Bzz1 results in a higher level of Bzz1 binding to Las17, it does not decrease the amount of Sla1 bound to Las17 (Figure 4). This means that Bzz1 must activate the SLAC complex without dissociating it. We propose a rearrangement of the SLAC complex that moves Sla1 off of the LGM just enough for G-actin to bind and predict that Bzz1 becomes a part of the SLAC complex rather than dissociating it.

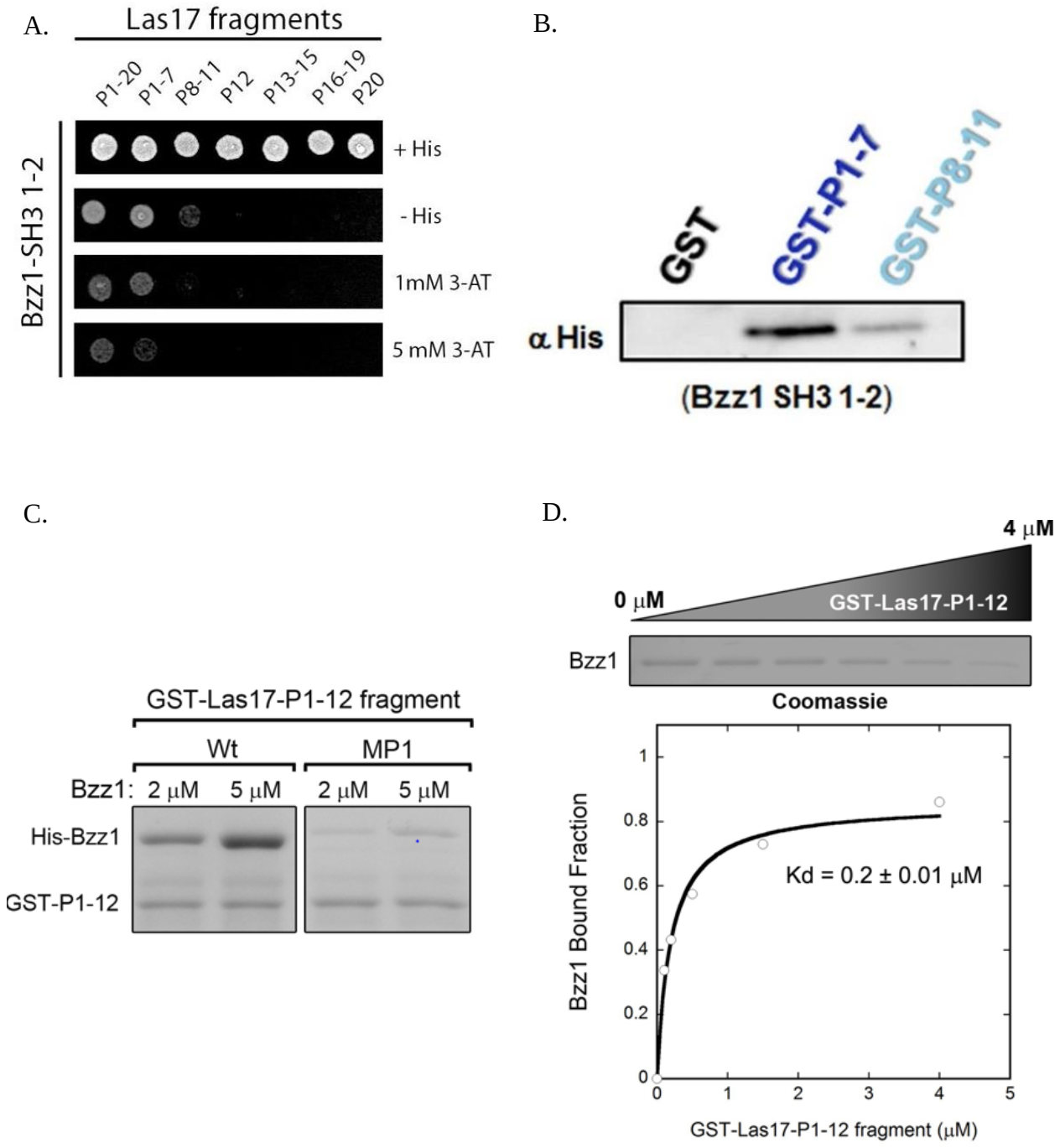

Figure 3. Characterizing the interaction between Las17 and Bzz1. (A) Yeast two-hybrid experiments showing the fragments of Las17 that interact with Bzz1 SH3 domains. (B) GST pulldown experiment showing a direct interaction. Bzz1 SH3 domains are visualized by Western blot using α-His antibodies. (C) Mutating P1 of Las17 depletes binding to Bzz1. Proteins stained with coomassie. (D) The K_D of Las17 and Bzz1 is in the sub-micromolar range. The amount of Bzz1 left in the supernatant was analyzed with ImageJ software and is shown with coomassie stain above the graph.

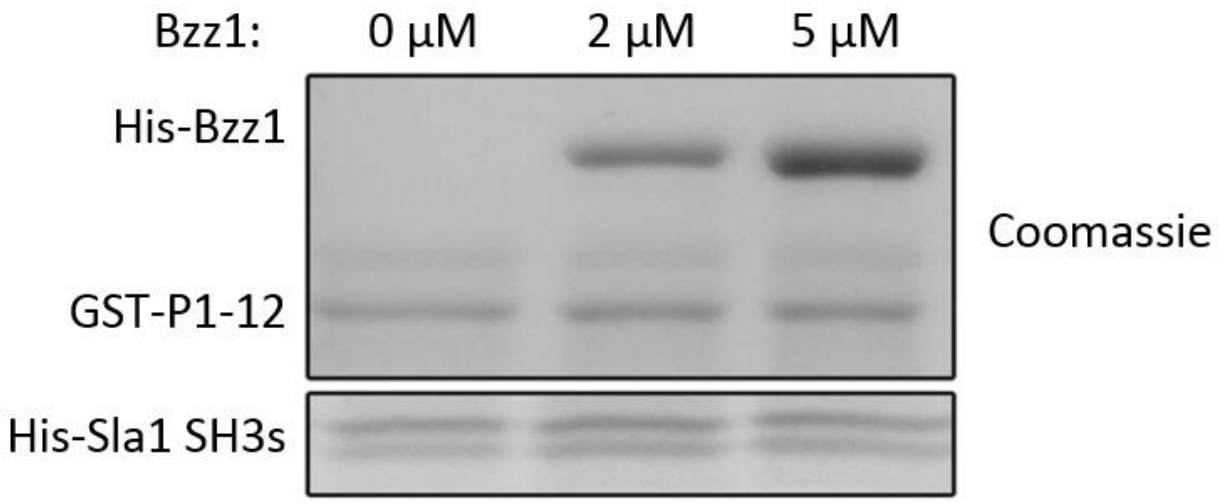

Figure 4. Bzz1 binds Las17 without inducing SLAC dissociation. Increasing the concentration of Bzz1 does not decrease the amount of Sla1 bound to Las17. Proteins are visualized with coomassie stain.

Bzz1 Binds Sla1

At this point, we wanted to test for a mechanism that supported the new idea that Bzz1 rearranges the SLAC complex. A preliminary GST pulldown showed that Bzz1 binds Sla1 (not shown). Upon inspection of the sequence of Bzz1, we found that a polyproline motif lies within the small linker in between the SH3 domains of Bzz1. To characterize this interaction, we created GST constructs of the following proteins: Bzz1 full length, Bzz1 with both SH3 domains deleted, and Bzz1 with the polyproline sequence of interest mutated (PxxP to AAxP) (Figure 5A). Upon binding to glutathione beads, each GST-Bzz1 fusion protein and GST alone was incubated with saturating amounts of poly-Histidine tagged Sla1 SH3 domains 1 and 2 (Sla1 SH3s). The bound fraction was analyzed by immunoblotting with anti-poly-His antibodies (Figure 5B). Again, full length Bzz1 binds Sla1. However, all binding is lost without the C-terminus of Bzz1. Furthermore, mutation of just the PxxP motif prevents the interaction just as much as the deletion of the C-terminus (Figure 5B). This data suggests a triad of interaction between Las17, Sla1, and Bzz1 and further supports the idea of SLAC complex rearrangement. Even so, it was not known whether this interaction was necessary for Bzz1 to activate the SLAC complex.

The Interaction between Bzz1 and Sla1 is Necessary for Activation of the SLAC Complex

Pyrene-actin polymerization assays are extremely useful experiments for measuring the potential of different proteins to activate or inhibit actin polymerization *in vitro*. Our experiments focus on Arp2/3-dependent polymerization and its activation by Las17. In short, pyrene-actin is added to a reaction containing the proteins of interest and polymerization is followed as an increase in pyrene fluorescence. When 75 nM Arp2/3, 75 nM Las17 full length, and 2 µM Actin are combined, high levels of polymerization are observed (Figure 6). As

A.

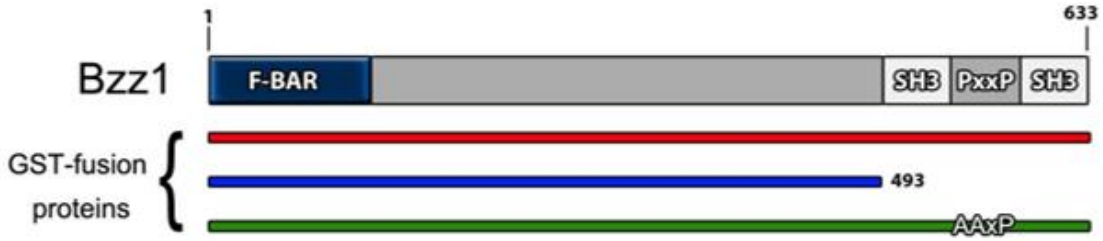

B.

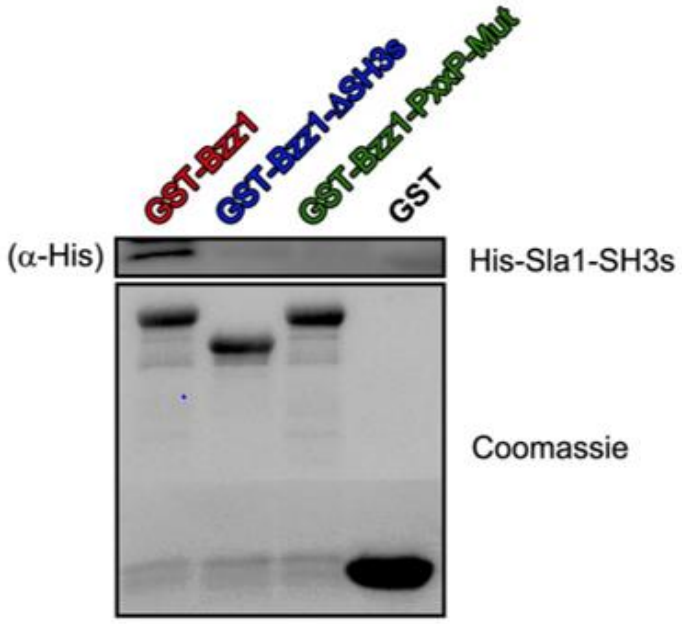

Figure 5. Bzz1 binds Sla1. (A) Full length Bzz1 is pictured above along with each of the constructs that were used in the binding assay. (B) The Bzz1 proteins and GST can be viewed by coomassie. Histidine tagged Sla1 SH3 1-2 domains were visualized by Western blot using α-His antibodies.

expected, the addition of 150 nM Sla1 SH3 1-2 domains drops this level of polymerization. Further, addition of 500 nM wild type Bzz1 recovers actin polymerization almost to the level observed without Sla1. However, equal amounts of the Bzz1 protein that cannot bind Sla1, Bzz1 AAxP, cannot recover the loss of polymerization accompanied by the addition of Sla1 (Figure 6). Although this experiment needs to be repeated, the existing data suggests that the interaction between Sla1 and Bzz1 is necessary for activation of actin polymerization *in vitro.*

These results must be confirmed *in vivo*. Thus, two strains of yeast were created to corroborate the pyrene-actin polymerization assay data. These strains have Las17 tagged with GFP using a histidine marker and Abp1 tagged with RFP using a tryptophan marker. Abp1 is a well-established marker of filamentous actin. One strain contains the Bzz1 PxxP to AAxP mutation and the dynamics of endocytic sites, or patches, were compared to the wild type strain containing the same tags. For this purpose live yeast cells were observed with a spinning disk confocal microscope. The patch lifetime of Las17 increased from 31.4 ± 1.0 s (wild type strain) to 40.1 ± 1.2 s (AAxP strain), exhibiting a p-value less than 0.0001 (Figure 7). The patch lifetime of Abp1 increased only slightly, from 18.3 ± 0.4 s to 19.4 ± 0.7 s, exhibiting a p-value of 0.1677. Importantly the time between the arrival of Las17 and the arrival of Abp1/actin, or delta time, increased from 16.4 ± 0.4 s to 25.0 ± 0.8 s, exhibiting a p-value less than 0.0001 (Figure 7). This data suggests that when Bzz1 cannot bind Sla1, Las17 remains inactive for a longer period of time. As a result, the onset of actin polymerization is significantly delayed. Initially, we attributed this delay to a defect in the ability of Bzz1 to activate Las17 NPF activity. However, it could also be caused by a defect in the recruitment of Bzz1 to sites of clathrin-mediated endocytosis. To understand what exactly was causing this defect another strain was generated and analyzed.

A.

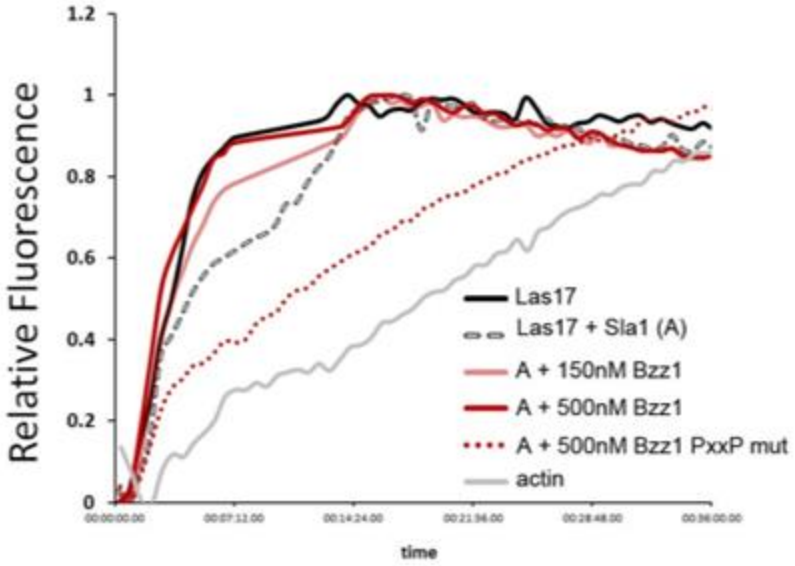

B.

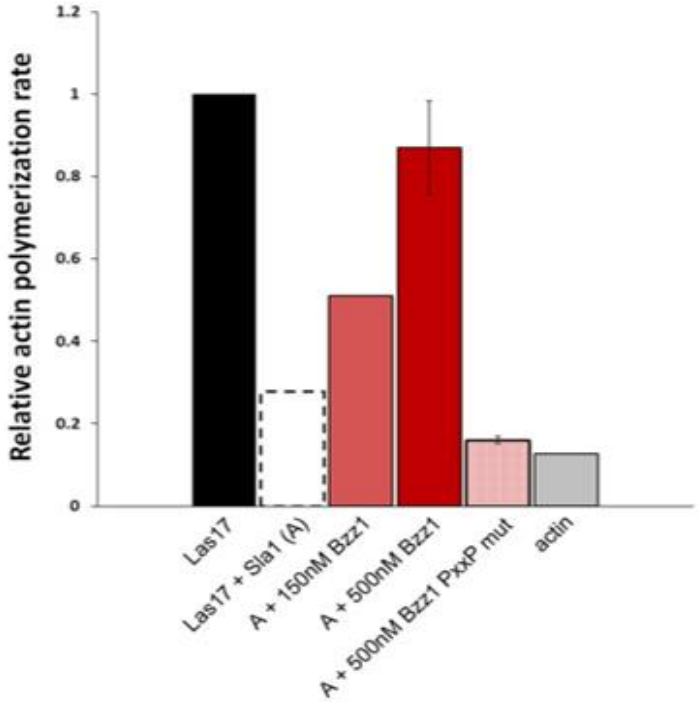

Figure 6. The PxxP to AAxP mutation depletes ability of Bzz1 to relieve Sla1 inhibition of Las17. (A) Levels of pyrene-actin fluorescence were measured using an excitation wavelength of 365 nm and an emission wavelength of 406 nm. All reactions contained: Arp2/3 complex (75nM), Las17 full length (75 nM), and pyrene-actin (2 µM). Also, Sla1 SH3 1-2 (150 nM), Bzz1 full length (150 or 500 nM), and Bzz1 PxxP mutant (500 nM) were added as indicated. (B) In order to truly determine the effect of the PxxP mutation on polymerization, the rates of polymerization were calculated using the slopes of the linear portions in graph A.

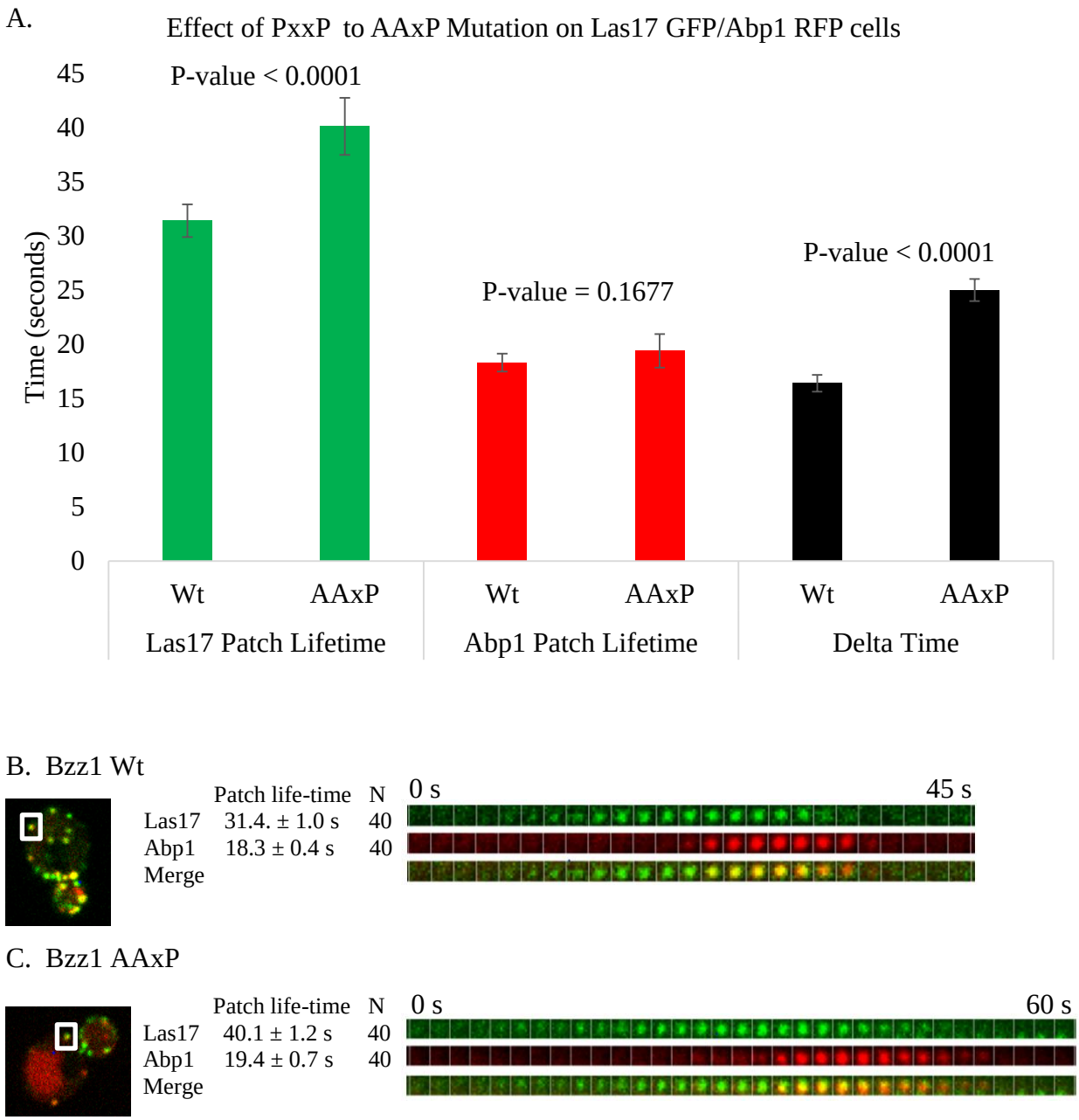

Figure 7. The PxxP to AAxP mutation affects the activation of Las17 and, by extension, the arrival of Abp1. (A) The graph depicts the average dynamics of 40 different patches and relevant p-values. (B/C) Kymographs of a typical endocytic patch in each strain. The cell and patch used for each kymograph can be seen on the left hand side.

The PxxP Mutation Affects Bzz1 Recruitment and Activator Capacity

Two more *Saccharomyces cervisiae* strains were created with Las17 tagged with GFP using a histidine marker, Abp1 tagged with RFP using a tryptophan marker, and Bzz1 wild type or Bzz1 AAxP tagged with iRFP using a kanamycin marker. These triple-tagged strains were analyzed by live cell fluorescence microscopy. Similar defects in Las17 patch lifetime (30.1 ± 1.29 s to 40.2 ± 1.73 s), Abp1 patch lifetime (15.8 ± 0.61 s to 16.8 ± 1.71 s), and Las17/Abp1 delta time (19.4 ± 1.21 s to 28.5 ± 1.36 s) were observed. This confirmed the results obtained with the double-tagged strains described above. By comparison, the patch lifetime of Bzz1 increased from 19.6 ± 1.11 s (wild type) to 23.7 ± 1.63 s (PxxP to AAxP mutant), exhibiting a p-value of 0.0452. The delta time for Las17 and Bzz1 increased from 14.3 ± 0.81 s to 19.2 ± 0.88 s, exhibiting a p-value of 0.0001 (Figure 8). Because the Las17/Abp1 delta time increases by about 10 seconds and the Las17/Bzz1 delta time increases by about 5 seconds, it is probable that the PxxP to AAxP mutation causes both a defect in Bzz1 recruitment and the ability of Bzz1 to activate actin polymerization. Kymographs illustrate that the arrival of Abp1 in the mutant strain is delayed by the slow arrival of Bzz1 and the decreased activity of Bzz1 once it arrives at the plasma membrane (Figure 8).

The N-terminus of Bzz1 is required for Activation

Thus far, we had focused on the importance of the C-terminus of Bzz1 and the interactions that occur at this end of the protein. The N-terminus of Bzz1 may be just as crucial for its function as an activator of CME. To test this possibility, we carried out another pyrene-actin polymerization assay that was very similar to the assay performed in figure 6. In this experiment, the activation capacity of the SH3 domains of Bzz1 was compared to that of Bzz1 full length. As expected, increasing concentrations of Bzz1 full length relieves the inhibition of

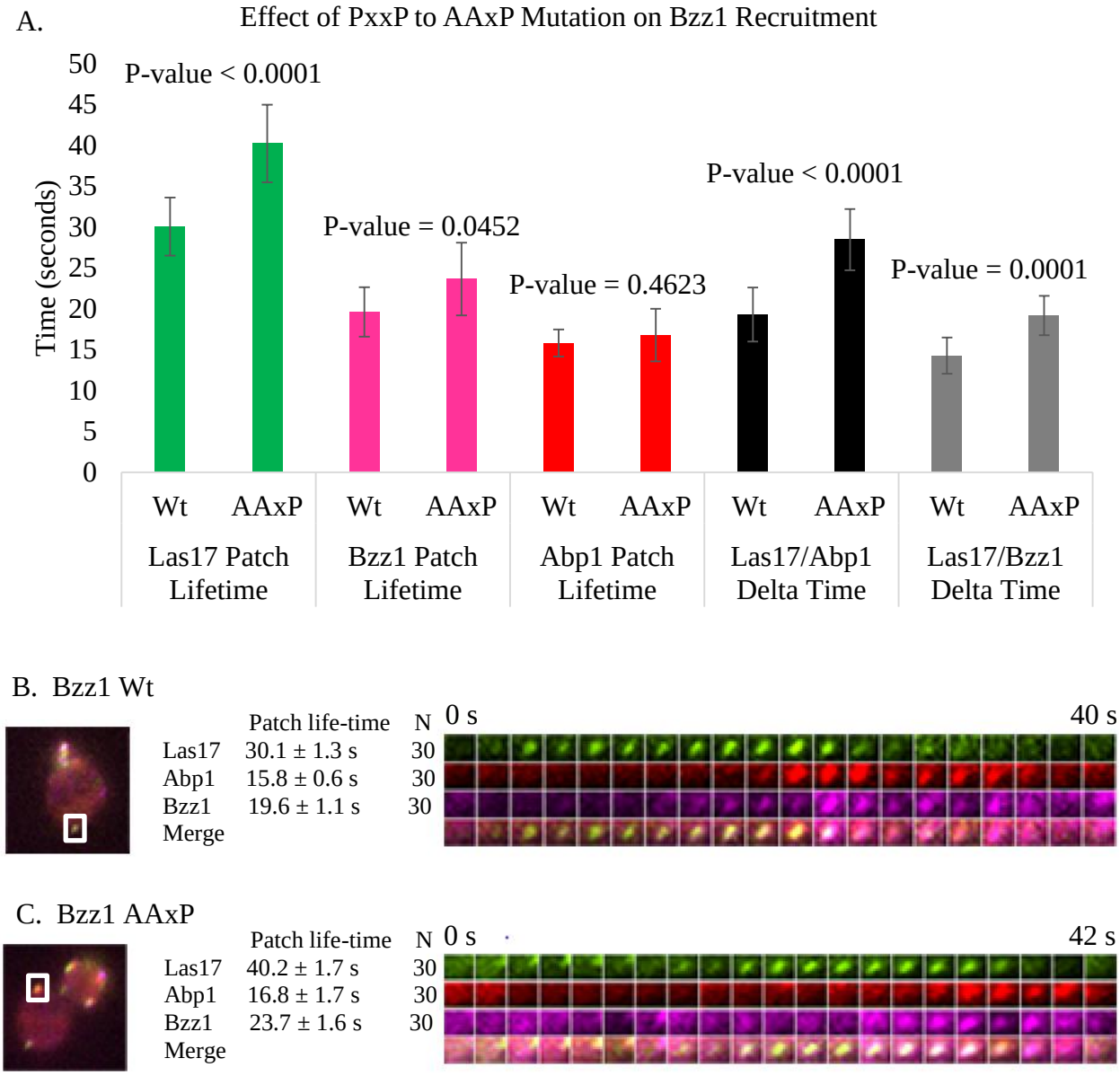

Figure 8. The AAxP mutation affects Bzz1 recruitment and activator capacity. (A) The graph shows the average dynamics of 30 different patches and relevant p-values. (B/C) Kymographs of a typical patch in each strain. Notice the extremely long delay between the arrival of Las17 and the arrival of Abp1. The cell and patch used for each kymograph can be seen on the left hand side.

Sla1 on Las17 and increases the rate of Arp2/3-mediated actin polymerization. Remarkably, adding the SH3 domains of Bzz1 inhibits actin polymerization (Figure 9). This proves that the N-terminus contains some characteristic that enables Bzz1 to function as an activator. As mentioned previously, the N-terminus of Bzz1 contains an F-BAR domain that is capable of both dimerizing, binding the phospholipids in the plasma membrane, and eliciting and supporting further curvature of the plasma membrane. It seems that this F-BAR domain also enables the SH3 domains of Bzz1 to participate in activation rather than competing with Sla1 and G-actin for the same site on Las17. However, the mechanism by which this occurs remained completely unknown.

Bzz1 Behaves like Syndapin

The mammalian homolog of Bzz1, Syndapin, can only adopt an active, open conformation when the SH3 domain binds to the proline-rich domain of the endocytic protein Dynamin (Figure 10A). To confirm whether or not Bzz1 behaves like Syndapin, a binding assay was designed. In this assay, 50 µg GST or GST Bzz1 F-BAR domains was allowed to bind glutathione beads in a 1000 µL reaction. Samples were washed and 150 µg poly-Histidine tagged Bzz1 SH3 domains or poly-Histidine tagged Sla1 SH3 1-2 domains (control) was added and allowed to bind in a 500 µL reaction. As observed by coomassie and α-His immunoblotting, the SH3 domains of Bzz1 bind the F-BAR domain of Bzz1 (Figure 10B). This mimics the behavior of Syndapin. It is also clear that the interaction between these two domains is specific; the F-BAR domain of Bzz1 does not bind the SH3 domains of Sla1 (Figure 10B). With the knowledge that Bzz1 can adopt the same, closed conformation as Syndapin, our next objective was to find out which protein plays the role of Dynamin for Bzz1. Las17 and Sla1 seem to be formidable candidates.

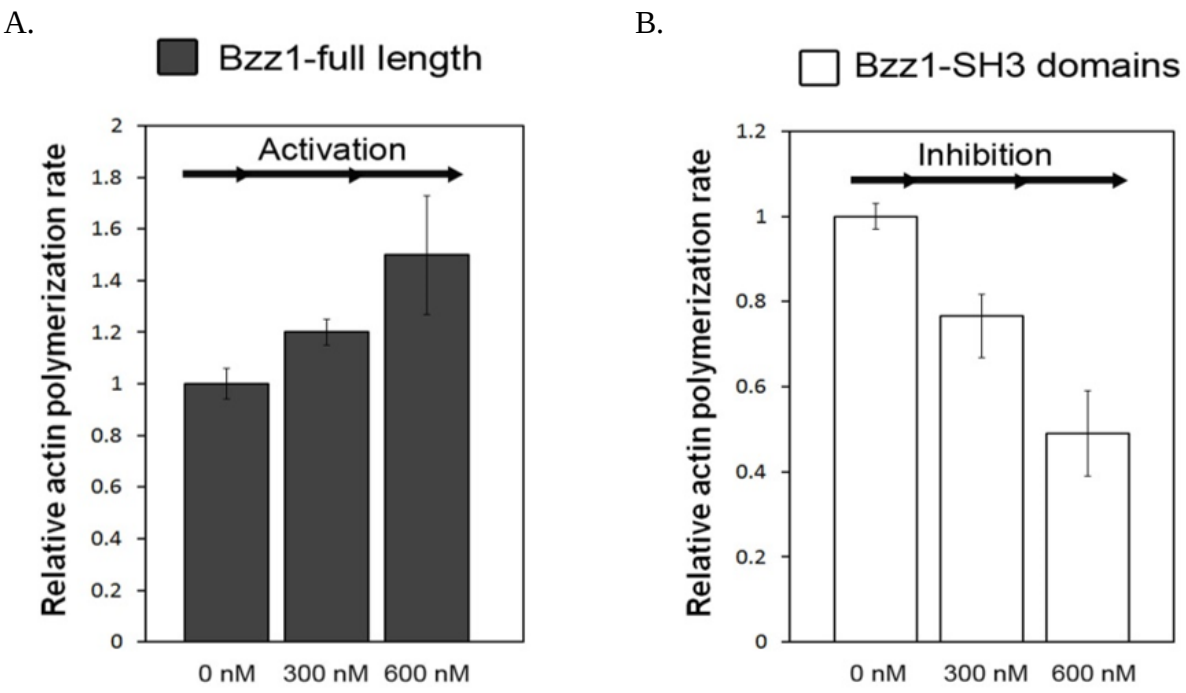

Figure 9. The N-terminus of Bzz1 is required for activation of actin polymerization. These reactions include: Las17 (75 nM), Arp2/3 (75 nM), Sla1 SH3 1-2 (150 nM), pyrene-actin (2 µM), and various concentrations of Bzz1 full length or Bzz1 SH3 domains. (A) The concentration of Bzz1 full length is proportional to the rate of actin polymerization. (B) The concentration of the SH3 domains of Bzz1 is inversely proportional to the rate of actin polymerization.

Bzz1 Changes the Shape of Liposomes

Liposomes are a resourceful way to study the *in vitro* effects of proteins that bind and/or mold the plasma membrane (6, 23). Before adding multiple proteins into this experiment we wanted to compare the capacities of Bzz1 full length and Bzz1 ΔSH3s to deform/tubulate the plasma membrane. The idea being that Bzz1 ΔSH3s will always exist in an open, active conformation, and will therefore behave like full length Bzz1 if it was bound to and activated by another protein. Liposomes were generated following a published procedure (11) and incubated with the lipid-binding dye, FM-4-64, to facilitate visualization by fluorescence microscopy (Figure 11). The liposomes were incubated with 5 µM of each protein for ten minutes at room temperature. To quantify, a 30 µm x 30 µm border was placed in the top right corner of each image. To be considered, a liposome had to be at least 1 µm in diameter. A total of 100 liposomes were analyzed per situation, each one deemed as either round and "regularly" shaped or misshapen and "tubule-containing." As a control, liposomes were incubated with buffer instead of protein and imaged. In this case 75% of the liposomes were considered round and regularly shaped while 25% of the liposomes were considered misshapen. 66% of the liposomes that were incubated with Bzz1 full length were round and regularly shaped while 34% of the liposomes were misshapen. 44% of the liposomes that were incubated with Bzz1 ΔSH3s were round and regularly shaped while 56% of the liposomes were misshapen (Figure 11A). These results suggest that Bzz1 has an increased ability to mold the plasma membrane when the F-BAR domain is unoccupied by the SH3 domains. Bzz1 full length still exhibits some ability to deform liposomes. Perhaps Bzz1 can adopt an open conformation, to some extent, without the help of other proteins.

A.

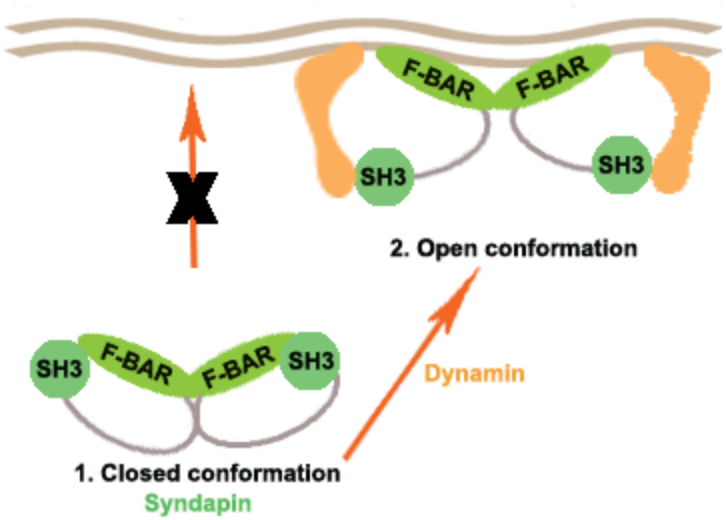

B.

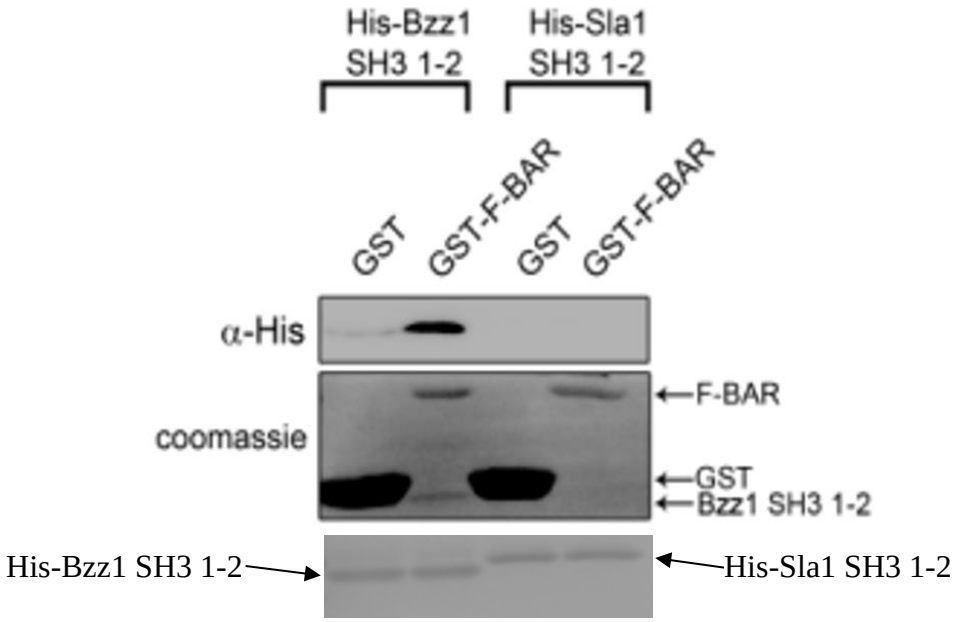

Figure 10. Bzz1 behaves much like its homolog in that the F-BAR domain can intramolecularly bind the SH3 domains. (A) This figure illustrates how Syndapin exists in a closed conformation until Dynamin binds the SH3 domain of Syndapin and elicits an open conformation that is capable of binding and tubulating the plasma membrane (12). (B) The Western blot near the top of this figure uses α-His antibodies to show that the SH3 domains of Bzz1 bind the F-BAR domain of Bzz1 while the SH3 domains of Sla1 do not. This result is confirmed by the coomassie gel below that. The coomassie gel at the very bottom shows input (1.5 µg) of both poly-Histidine tagged Bzz1 SH3 domains and poly-Histidine tagged Sla1 SH3 1-2 domains.

A.

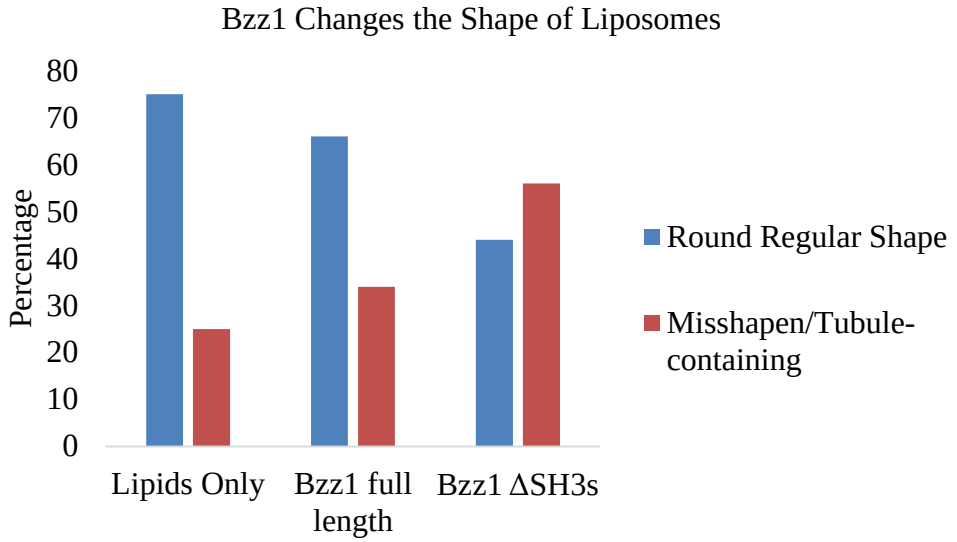

B.

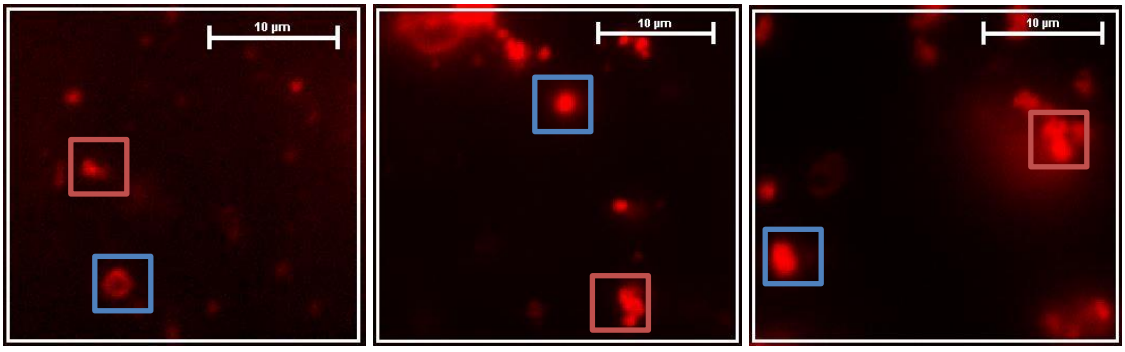

Lipids Only Bzz1 full length Bzz1 ΔSH3s

Figure 11. Bzz1 can change the shape of liposomes. (A) The percentage of round, regularly shaped liposomes and misshapen, tubule containing liposomes in each situation. (B) Fluorescence microscopy images for each situation were obtained using a 561 nm laser and a 100 ms exposure. Examples of regularly shaped liposomes are outlined in blue. Examples of misshapen liposomes are outlined in red.

Deformation of Liposomes is an effect of Bzz1 Binding

In order to be sure that the change in liposome shape is a specific effect of the interaction with Bzz1 proteins and not just a result of adding any protein in general, a liposome binding assay was carried out. Liposomes were incubated with the same amount of Bzz1 full length, Bzz1 ΔSH3s, and Bzz1 SH3s. Similar amounts of protein were found in the supernatant and pellet fractions of samples that did not contain liposomes (Figure 12). Upon the addition of liposomes, several changes occurred. Bzz1 ΔSH3 has the highest amount of protein in the pellet fraction, 85.6%. This suggests that this protein has the highest affinity for the liposome and the greatest capacity to mold the plasma membrane. Bzz1 full length is not far behind, though, with 74.4% of the protein added existing in the pellet fraction. This decreased interaction in comparison to Bzz1 ΔSH3s could explain the lower percentage of misshapen liposomes in the microscopy data. As a negative control, the SH3 domains behave as expected, with no significant change in supernatant and pellet fractions upon the addition of liposomes. This experiment confirms what we have seen in our microscopy experiments and shows that the *in vivo* increase in delta time between Las17 and Bzz1 AAxP is not due to lipid binding but rather the interaction of Bzz1 with other proteins.

Explaining the Misshapen Characteristic of Liposomes

Originally, the goal of the liposome experiments was to test whether different versions of Bzz1 and Bzz1 in the presence of a binding partner can deform/tubulate a membrane. In this way we could provide evidence that the actin polymerization and tubulation activity of Bzz1 may be coupled. However, quantifying regular and misshapen liposomes is admittedly somewhat ambiguous. Does misshapen/tubule-containing mean that the protein is creating membrane protrusions that are budding off of the liposomes or is the protein bringing multiple liposomes

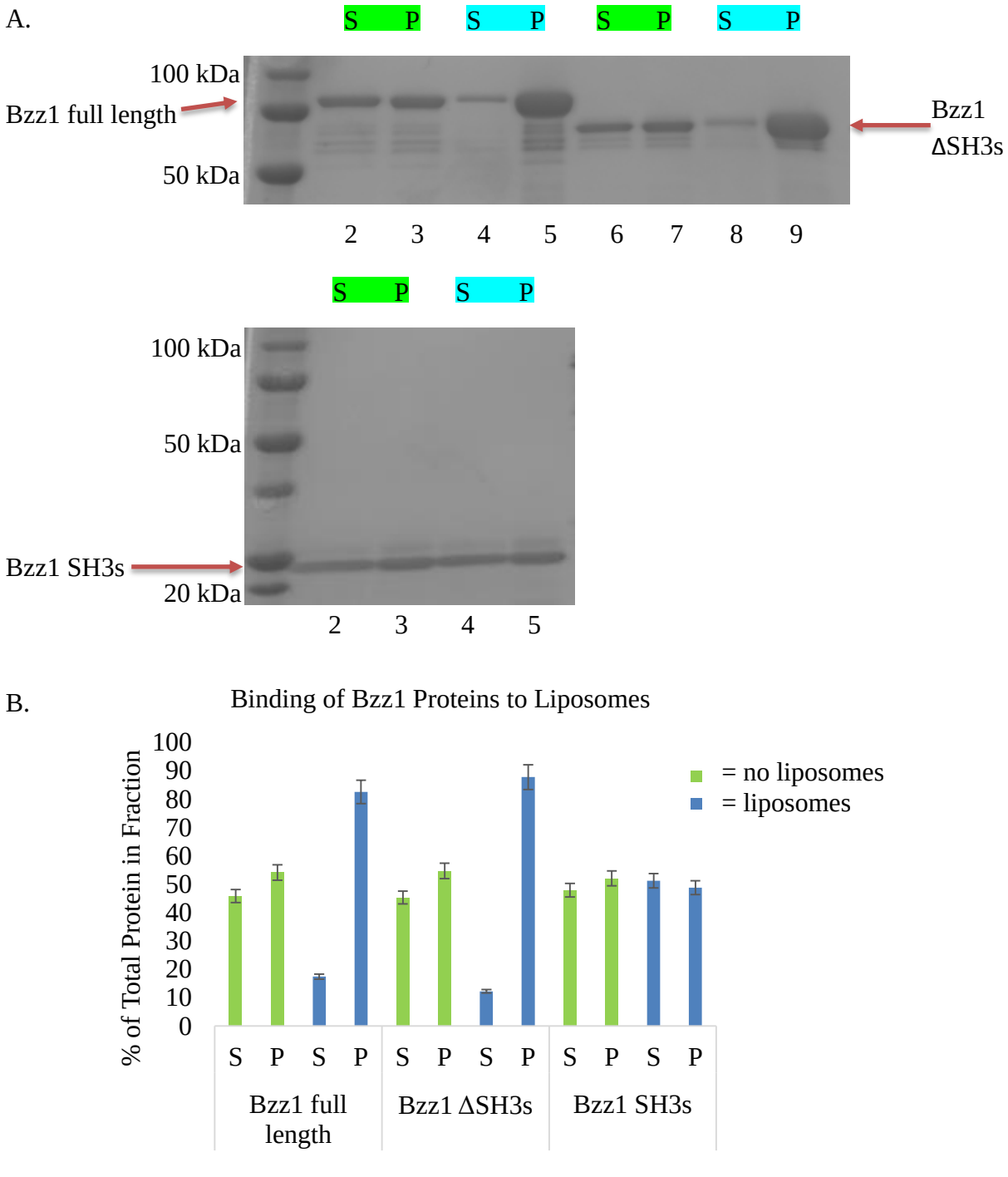

Figure 12. Bzz1 binds liposomes. (A) Coomassie stained gels showing the amount of Bzz1 full length, Bzz1 ΔSH3s, and Bzz1 SH3s in the supernatant (S) and pellet (P) fractions of samples without (wells 2, 3, 6, and 7) and with liposomes (wells 4, 5, 8, 9). (B) Protein amounts were quantified using ImageJ and divided by the total amount of protein to show the percent of protein in each fraction.

together? In an effort to better investigate this point, we are making Bzz1 constructs tagged with poly-Histidine and GFP in order to purify from *E. coli* and visualize by fluorescence microscopy, respectively. Bzz1 full length was successfully tagged and purified, while Bzz1 ΔSH3s is in progress. Bzz1 full length GFP has been incubated with liposomes and imaged. In support of previous data, Bzz1 diffusely colocalizes with the liposomes (Figure 13). However, without the ΔSH3s construct to compare, it is difficult to speculate how much Bzz1 full length is binding to the liposomes and where exactly that interaction is occurring. Because the ΔSH3s construct has been shown to elicit a higher percentage of misshapen liposomes as well as higher affinity for liposomes, we predict that there will be a higher and more concentrated GFP signal on liposomes incubated with this protein. It is our next priority to test this prediction experimentally. If this experiment is performed successfully, the prospect of adding more proteins into the mix would be more feasible. Eventually, we would like to asses actin polymerization by Arp2/3, Las17, Sla1, and Bzz1 while monitoring the capacity of Bzz1 to deform the membrane.

Creating a Model that Integrates the New Data

With all of this new data, it is important to combine it all together in a comprehensive model that illustrates what we think is actually happening. This model, however oversimplified, provides a clear picture of how Bzz1 might couple actin polymerization and membrane tubulation in two steps (Figure 14). In step one, the SLAC complex exists at the plasma membrane and the SH3 domains of Sla1 are blocking G-actin from binding Las17. Bzz1 exists in a homodimer form and the F-BAR domains are fully inhibited by the SH3 domains. In step two, the SH3 domains of one subunit are binding the P1 site of Las17 with a strong affinity. The SH3 domains of the other subunit are occupying the F-BAR domain, partially preventing the dimer from binding the plasma membrane. Between step two and step three, the SH3 domains

A.

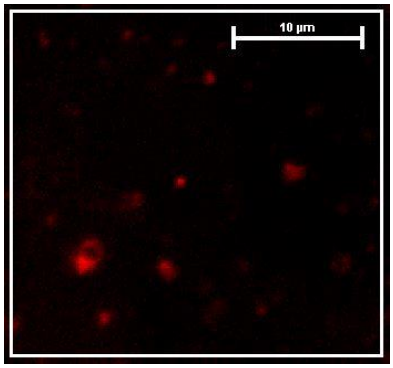

B.

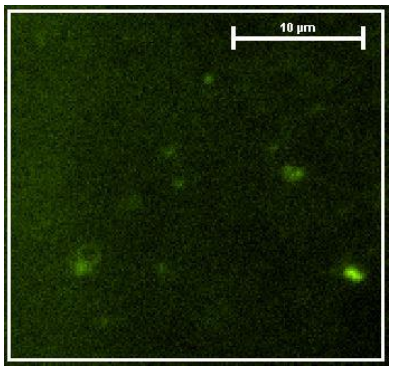

C.

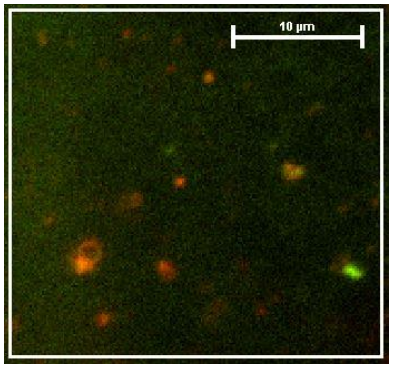

Figure 13. Bzz1full length GFP colocalizes with liposomes. (A) Image obtained of liposomes using the 561 nm laser. (B) Image obtained of Bzz1 GFP using a 473 nm laser. (C) Merge of images A and B.

on right “arm” of Bzz1 could be circulating between two binding sites, the LGM and the F-BAR domain. It is the LGM domain that could bring the polyproline motif of Bzz1 into proximity with the SH3 domains of Sla1. This leads to step three. The PxxP motif of Bzz1 binds Sla1 SH3 1-2 domains and partially pulls it off of the LGM. This allows G-actin to bind without dissociating the SLAC complex. In addition, both of the F-BAR domains are unoccupied, allowing Bzz1 to deform the plasma membrane (Figure 14).

This model nicely correlates with another model published by the Di Pietro laboratory that illustrates both the LGM and the WH2 domain of Las17 feeding G-actin to Arp2/3 which is bound to the acidic tail of Las17 (8). There are additional experiments to be performed in order to further validate this model. This model is supported by our existing data, however our data does not disagree with the prediction that dimerization of the F-BAR domains of Bzz1 could allow Bzz1 to gather two molecules of Las17 together, multiplying the NPF effects. It is important that we consider both models without bias. In addition, we are not limiting our model to Las17, Sla1, and Bzz1. We embrace the possibility that other proteins are a part of the mechanism described.

Step 1:

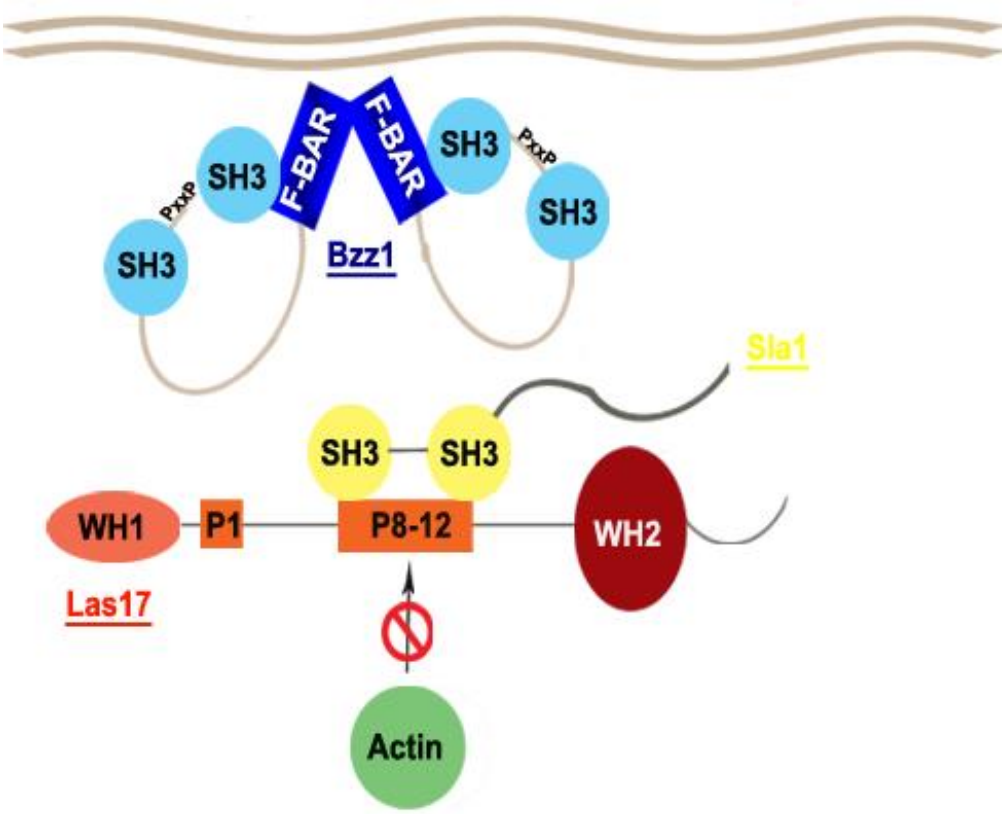
F-BAR
F-BAR
SH3
SH3
SH3
SH3
PxxP
PxxP
Bzz1
Sla1
SH3
SH3
WH1
P1
P8-12
WH2
Las17
Actin

Step 2:

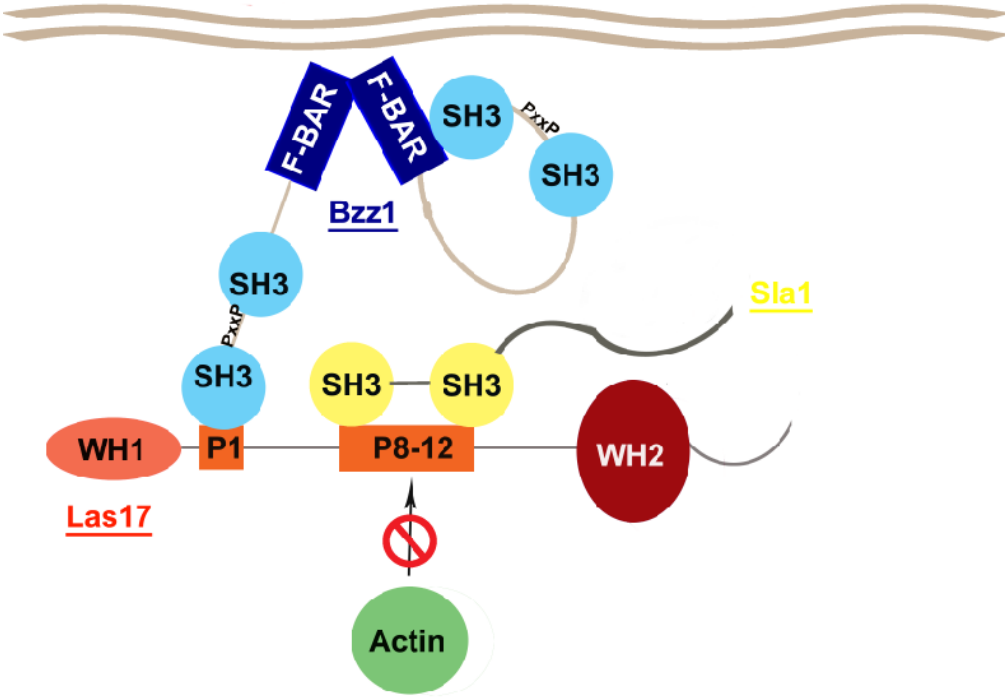
F-BAR
F-BAR
SH3
SH3
PxxP
Bzz1
SH3
PxxP
Sla1
SH3
SH3
SH3
WH1
P1
P8-12
WH2
Las17
Actin

Step 3:

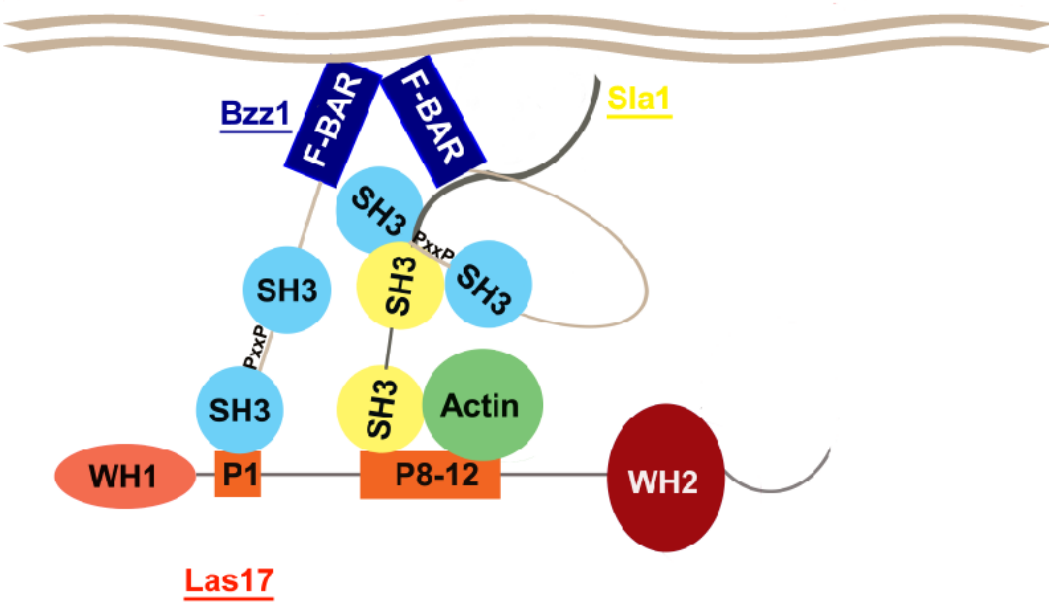

Figure 14. The mechanism by which Bzz1 activates actin polymerization and tubulates the plasma membrane.

DISCUSSION

Clathrin-mediated endocytosis depends heavily on the polymerization of actin to form a network that drives the clathrin coated vesicle into the cytosol. Before this research it was known that Sla1 inhibits the NPF activity of Las17 by blocking G-actin binding at the LGM. Our biochemical analyses have shown that Bzz1 alleviates this inhibition. Surprisingly, the mechanism of activation by Bzz1 does not require dissociation of the SLAC complex. Instead Bzz1 becomes a part of the complex, possibly rearranging it in a way that allows G-actin to bind. We have also shown that Bzz1 and Sla1 interact and have provided *in vitro* data that suggests that this interaction is necessary for the role of Bzz1 as an activator. Our *in vivo* data further supports this idea. The interaction between Bzz1 and Sla1 is also necessary for well-timed recruitment of Bzz1 to the plasma membrane.

We have also begun to explore additional roles for Bzz1 during clathrin-mediated endocytosis. F-BAR domains have been shown to dimerize. Proteins containing this domain can arrange around a clathrin coated pit and both support existing curvature and elicit further tubulation. We show that Bzz1, like Syndapin, could exist in a closed conformation that inhibits the F-BAR domain and an open conformation that allows the F-BAR domain to bind and tubulate the plasma membrane. Our liposome experiments validate this idea. Bzz1 can better bind and deform the plasma membrane when the F-BAR domain is unoccupied by Bzz1 SH3s.

We tried to fit this new data into a model that encompasses existing research and our new research. Nevertheless, questions remain unanswered and we continue to strive for answers. For instance, our model implies that dimerization is necessary for activation of actin polymerization by Bzz1. This can be tested using a pyrene-actin polymerization assay that compares the activation capacity of Bzz1 full length, MBP tagged Bzz1 ΔF-BAR, and GST tagged Bzz1 ΔF-

BAR. The GST tag is also capable of dimerizing; thus, any activation lost upon the deletion of the F-BAR domain, can presumably be rescued when replaced by another dimerizing mechanism. Because the MBP tag is monomeric, dimerization and activation would not be rescued. Another experiment that would help to refine our model is to image liposomes with GFP tagged Bzz1 ΔSH3s. Hopefully this will provide a clearer idea as to how exactly Bzz1 deforms the plasma membrane. We would also like to image liposomes with Bzz1 full length and a binding partner such as Sla1 or Las17. It might be that binding of the SH3 domains to another protein has the same effect as deleting the SH3 domains.

To add to the complexity of this research, there are additional proteins that have been shown to interact with Las17, Sla1, and/or Bzz1. Syp1 also inhibits Las17, but departs from the actin patch before the arrival of actin. Could the arrival of Bzz1 be a cue for the departure of Syp1? Ysc84 could also play a major role in this mechanism. From its N to C-terminus, Ysc84 contains a YAB (Yeast actin binding) domain, a linker domain, and one SH3 domain that binds both Sla1 and P12 of Las17 (1). This interaction with P12 activates the YAB domain of Ysc84 to bind and bundle existing actin filaments (19). With this information, it is not hard to imagine the role that other proteins might play in this mechanism.

Although we continue to come up with more questions, we have begun to answer a few questions that researchers have been asking for a while now, and the roles of Bzz1 in clathrin-mediated endocytosis are now clearer than before.

MATERIALS AND METHODS

Protein Purification

GST-fusion and poly-Histidine-fusion proteins were expressed in *Escherichia coli* (BL21) and affinity purified using glutathione-sepharose-4B affinity resin or TALON cobalt affinity resin, respectively. All proteins were dialyzed in 10 mM Tris Buffer.

Pyrene-actin Polymerization Assay

Pyrene-actin polymerization assays were performed with 2.0 µM rabbit actin, 75 nM Arp2/3 complex, 75 nM Las17, 150 nM Sla1 SH3 1-2, and 500 nM Bzz1 (wild type or mutant). To eliminate nuclei, pyrene-actin was incubated in G-Buffer (10 mM Tris pH 8.0, 0.2 mM $CaCl_2$, 0.2 mM ATP, 0.2 mM DTT) on ice for 1.5 hours and centrifuged at 95,000 rpm in a TLA100.3 rotor at 4°C for 1.5 hours. These proteins were added to a 96 well plate. Following the addition of polymerization buffer (500 mM KCl, 10 mM ATP, 20 mM $MgCl_2$), actin polymerization was measured for approximately 1 hour using a microplate reader (exc. 365 nm, emis. 406 nm). Data was normalized by subtracting values from a well containing actin and no polymerization buffer and dividing by the maximum value in all the wells. Polymerization rates were calculated from the slope of the linear part of the curves obtained.

Liposome Experiments

Phosphatidyl inositol and phosphatidyl choline were suspended in 98% chloroform 2% methanol solution to yield a final concentration of 10 mmol/L and stored at -20°C. 10 µL of each lipid was added to an eppendorf tube and dried under a steady flow of nitrogen gas. The lipids were then dried in a SpeedVac for 2 hours. 20 µL of 250 mM Sucrose was added. The lipids were incubated at 50°C for 1.5 hours and agitated every 15 minutes within this incubation. 380 µL of Buffer A (25 nM Tris pH 8.0, 50 mM KCl) was added to the lipid/sucrose mixture and

stored at 4°C. For imaging, equal parts FM-464 dye and prepared lipids were mixed and injected into a makeshift chamber. 1-5 µM of the protein of interest was incubated with the lipid/dye mixture before imaging.

Liposome Binding Assay

Liposomes were prepared as described above, except the dye was replaced with Buffer A. 80 µL of this prep was incubated with 10 µg of each protein (totaling 100 µL) for 15 minutes at room temperature. In the sample containing no liposomes, 80 µL of Buffer A was used. The samples were centrifuged at 16,000 g for another 15 minutes at room temperature. The top 85 µL was collected as the supernatant fraction and the remaining 15 µL was the pellet fraction. Fractions were run on an SDS-PAGE gel, visualized with coomassie stain, and analyzed using ImageJ software (11).

Fluorescence Microscopy

Fluorescence microscopy was performed using a Nikon Eclipse Ti microscope with ANDOR iXon3 camera or an Olympus Ix81 spinning-disk confocal microscope with Photometrics Cascade II camera and a 100x objective. Cells were imaged during log phase and time-lapse images were created by taking 200 images at a 600 ms interval. NISAnalysis Software or SlideBook 6.0 was used to determine patch lifetimes and delta times.

Yeast two-hybrid analysis

For yeast two-hybrid analysis, Bzz1 SH3 1-2 was fused to the Gal4p activation domain by subcloning from a PGEX-5x-1 plasmid to the pGAD424 plasmid. Las17 fragments were fused with the Gal4 DNA-binding domain by subcloning from a pET-30a plasmid to the pGBT9 plasmid. These constructs were tested for interaction by observing the level of growth on plates lacking Histidine and plates containing 1mM 3-AT or 3 mM 3-AT.

Immunoblotting

All of the Western Blots were carried out using the same protocol and antibodies. Samples were run on an SDS-PAGE gel and subsequently transferred onto a membrane. To avoid non-specific binding, the membrane was incubated with 5% milk and 0.5% Tween20 for 1 hour at room temperature. The membrane was then incubated with primary, α-His antibodies and 5% milk in a 1:3000 ratio overnight at 4°C. After three 5 minute washes with 1x PBS, the membrane was incubated with secondary, anti-mouse antibodies and 5% milk in a 1:3000 ratio for 1 hour at room temperature. Before imaging, the membrane was given three more 5 minute washes with 1x PBS and then incubated with ECL Prime Western Blotting Detection Reagent for 5 minutes at room temperature

Generation of Yeast Strains

In order to generate the double-tagged Bzz1 AAxP strain we had to first create an intermediated strain. We transformed Y371 (Las17 GFP (His), Abp1 RFP (Trp)) with a construct containing the URA3 gene and the 3' UTR of Bzz1 and plated on –URA plates. Colonies were sequenced to check for the construct. This intermediate strain was then transformed with a pRS-315 (Leu) plasmid and a construct containing the AAxP mutation and the 3' UTR of Bzz1 and grown on plates lacking leucine. These colonies were transferred to 5FOA plates to ensure the removal of the URA3 gene and sequenced. Y371 (wild type) and Y580 (Las17 GFP (His), Abp1 RFP (Trp), and Bzz1 AAxP) were imaged in parallel to determine the effects of the PxxP to AAxP mutation on endocytic patch dynamics.

In order to create our triple-tagged strains we had to make another intermediate strain. Y087 (no tags) was transformed with a construct containing the URA3 gene and the 3' UTR of Bzz1. Colonies were grown on –URA plates, sequenced, and saved as Y618. This strain was

transformed with a pRS-315 (Leu) plasmid and a construct containing the AAxP mutation and the 3' UTR of Bzz1 and grown on plates lacking leucine. These colonies were transferred to 5FOA plates to ensure the removal of the URA3 gene, sequenced, and saved as Y626. Y087 and Y626 were transformed with a construct containing iRFP, a kanamycin marker, and a partial Bzz1 sequence. These colonies were grown on plates containing G418, sequenced, and saved as Y640 (Bzz1 iRFP (Kan)) and Y641 (Bzz1 AAxP iRFP (Kan)). Both of these strains were mated with Y371 and dissected, selecting for all three tags. Y643 (Bzz1 iRFP (Kan), Las17 GFP (His), Abp1 RFP (Trp)) and Y645 (Bzz1 AAxP iRFP (Kan), Las17 GFP (His), Abp1 RFP (Trp)) were imaged to determine the effect of the PxxP to AAxP mutation on the recruitment of Bzz1 to endocytic patches.

REFERENCES

(1) Dewar, H., Warren D. T., Gardiner F. C., et al. (2002) Novel Proteins Linking the Actin Cytoskeleton to Endocytic Machinery in *Saccharomyces cerevisiae. Mol. Biol. Cell.* 13, 3646-3661.

(2) Di Pietro S.M., et al. (2010) Regulation of clathrin adaptor function in endocytosis: novel role for the SAM domain. *EMBO J.* 29, 1033-1044.

(3) Drubin D.G., Kaksonen M., Toret C., Sun Y. (2005) Cytoskeletal networks and pathways involved in endocytosis. *Novartis Found Symp*. 269, 35-42.

(4) Doyon J.B., Drubin D.G., et al. (2011) Rapid and efficient clathrin-mediated endocytosis revealed in genome-edited mammalian cells. *Nat. Cell Biol.* 13(3), 331-337.

(5) Engqvist-Goldstein A.E., Drubin D.G. (2003) Actin assembly and endocytosis: from yeast to mammals. *Annu. Rev. Cell Dev.* 19, 287-332.

(6) Farsad K., Ringstad N., Takei K., Floyd S.R., Rose K., De Camilli P. (2001) Generation of high curvature membranes mediated by direct endophilin bilayer interactions. *J. Cell Biol*. 155, 193–200.

(7) Feliciano D., Di Pietro S.M. (2012) SLAC, a complex between Sla1 and Las17, regulates actin polymerization during clathrin-mediated endocytosis. *Mol. Biol. Cell.* 23(21), 4256-4272.

(8) Feliciano D., Tolsma T.O., Farrell K.B., Aradi A., Di Pietro S.M. (2015) A second Las17 monomeric actin-binding motif functions in Arp2/3-dependent actin polymerization during endocytosis. *Traffic*., in press.

(9) Galletta B.J., Chuang D.Y., Cooper J.A. (2008) Distinct roles for Arp2/3 regulators in actin assembly and endocytosis. *PLoS Biol.* 6, e1.

(10) Howard, et al. (2002) Sla1p serves as the targeting signal recognition factor for $NPFX_{(1,2)}D$-mediated endocytosis. *JBC.* 157(2), 315-326.

(11) Itoh T., Erdmann K.S., Roux A., Habermann B., Werner H., De Camilli P. (2005) Dynamin and the Actin Cytoskeleton Cooperatively Regulate Plasma Membrane Invagination by BAR and F-BAR Proteins. Dev. Cell. 9(6), 791-804.

(12) Mishra M., Huang J., Balasubramanian M.K. (2014) The Yeast Actin Cytoskeleton. FEMS Microbiol. Rev. 10.1111/1574-6976.12064.

(13) Moravcevic K., Lemmon M.A., et al. (2015) Comparison of Saccharomyces cerevisiae F-BAR Domain Structures Reveals a Conserved Inositol Phosphate Binding Site. Structure. 23(2), 352-63.

(14) Mullins R. D., Heuser J.A., Pollard T.D. (1998) The interaction of Arp2/3 complex with actin: nucleation, high affinity pointed end capping, and formation of branching networks of filaments. Proc. Natl. Acad. Sci. USA. 95, 6181–6186.

(15) Newpher T. M., Lemmon S.K. (2006) Clathrin is important for normal actin dynamics and progression of Sla2p-containing patches during endocytosis in yeast. Traffic. 7, 574-588.

(16) Padrick S.B., Rosen M.K. (2010) Physical mechanisms of signal integration by WASP family proteins. Annu. Rev. Biochem. 79, 707–735.

(17) Padrick S.B., Doolittle L.K., Brautigam C.A., King D.S., Rosen M.K. (2011) Arp2/3 complex is bound and activated by two WASP proteins. Proc. Natl. Acad. Sci. USA. 108, E472–E479.

(18) Rao Y., Ma Q., Vahedi-Feridi A., et al. (2010) Molecular basis for the SH3 domain regulation of F-BAR-mediated membrane deformation. PNAS. 107(18), 8213-8218.

(19) Robertson A., Allwood E., Smith A. S., et al. (2009) The WASP Homologue Las17 Activates Novel Actin-regulatory Activity of Ysc84 to Promote Endocytosis in Yeast. *Mol. Biol. Cell.* 20, 1618-1628.

(20) Rodal A.A., Manning A.L., Goode B.L., Drubin D.G. (2003) Negative regulation of yeast WASp by two SH3 domain-containing proteins. Curr. Biol. 13, 1000–1008.

(21) Sirotkin V., Beltzner C.C., Marchand J.B., Pollard T.D. (2005) Interactions of WASp, myosin-I, and verprolin with Arp2/3 complex during actin patch assembly in fission yeast. J. Cell Biol. 170, 637.

(22) Sun Y., Martin A.C., Drubin D.G. (2006) Endocytic internalization in budding yeast requires coordinated actin nucleation and myosin motor activity. Dev. Cell. 11, 33–4.

(23) Takei K., Haucke V., Slepnev V., Farsad K., Salazar M., Chen H., De Camilli P. (1998) Generation of coated intermediates of clathrin-mediated endocytosis on protein-free liposomes. Cell. 94, 131–141.

(24) Ti S.C., Jurgenson C.T., Nolen B.J., Pollard T.D. (2011) Structural and biochemical characterization of two binding sites for nucleation-promoting factor WASp-VCA on Arp2/3 complex. Proc. Natl. Acad. Sci. USA. 108, E463–E471.